Photoaffinity Cross-Linking of the Corticotropin-Releasing Factor Receptor Type 1 with Photoreactive Urocortin Analogues

Oliver Kraetke,*,‡ Brian Holeran,§ Hartmut Berger,‡ Emanuel Escher,§ Michael Bienert,‡ and Michael Beyermann‡

Department of Peptide Chemistry, Institute of Molecular Pharmacology (FMP), 13125 Berlin, Germany, and Department of Pharmacology, Faculty of Medicine, Université de Sherbrooke (IPS), Sherbrooke, Quebec, Canada J1H 5N4

Received April 18, 2005; Revised Manuscript Received September 29, 2005

ABSTRACT: Interaction of natural peptide ligands with class 2 GPCRs, which are targets of biologically important hormones such as glucagon, secretin, and corticotropin-releasing factor (CRF), occurs with a common orientation, in that the ligand C-terminus binds to the extracellular receptor N-terminus, whereas the ligand N-terminus binds to the receptor juxtamembrane domain. N-Terminal truncation, by eight amino acids in the case of CRF, leads to antagonists, suggesting those residues constitute the receptor activating sequence. Here, we identified by photoaffinity cross-linking using *p*-benzoyl-L-phenylalanine (Bpa) analogues of urocortin (Ucn) the most affine CRF receptor agonist, interaction domains of CRF_1 receptor with Bpa residues at exclusive positions. Specific cleavage patterns of the corresponding ligand−receptor complexes, obtained using several cleavage methods in combination with SDS−PAGE for fragment size determination, showed that a Bpa group located N-terminally or in position 12 binds at the second and such in position 17 or 22 at the first extracellular receptor loop. Our results indicate that the very N-terminal ligand residues (1−11), which are responsible for receptor activation, are oriented to the juxtamembrane domain by interaction of amino acid residues 12, 17, and 22. Our findings contradict a recently proposed interaction model derived from ligand interaction with a soluble receptor N-terminus, indicating that conclusions drawn from such a reduced system may be of limited value to understand the interaction with the full-length receptor.

Urocortin (Ucn)[1] is a 40 amino acid (aa) peptide, related to corticotropin-releasing factor (approximately 45% sequence identity to CRF), and was originally identified by Vaughan et al. (*1*) in mammalian midbrain. Urocortin plays a key role in the response of the cardiovascular system to stress, boosts memory modulating effects, and is involved the regulation of the appetite-feeding behavior (*1*−*3*). It interacts with comparable affinity with two pharmacologically different types of receptors, the corticotropin-releasing factor receptors type 1 and type 2 (CRF_1R, CRF_2R) including isoforms (*4*−*9*), which belong to class 2 of G-protein-coupled receptors (GPCRs). Recently, a third receptor type (CRF_3R) has been identified (*10*), which is highly homologous to CRF_1R, but relatively little is known about this receptor so far. CRF receptors are widely distributed in various mammalian tissues, mainly in the brain (*5*, *8*), and are involved in the natural body response to stress by acting through the hypothalamic−pituitary−adrenal axis on the stimulation of the production of proopiomelanocortin and secretion of adrenocorticotropic hormone (*11*−*13*). Thus, they are favored pharmacological targets for the development of new drug candidates with potential in clinical fields.

Elucidations of primary structures of numerous GPCRs have prompted investigators to identify specific ligand binding sites at the receptor, located at the receptor N-terminus and the juxtamembrane region, which relied on the use of indirect techniques such as chimeric receptors, deletion mutants, and mutagenesis. For CRF_1R, Perrin et al. (*14*) demonstrated with a series of mutant receptors that the extracellular domains, especially the N-terminus, are important for ligand binding. Furthermore, Dautzenberg et al. (*15*, *16*) localized a ligand binding domain within the CRF_1R N-terminus of *Xenopus laevis* to aa 70−89 by the use of chimeric receptors. Moreover, Wille et al. (*17*) and Assil et al. (*18*) underlined a role for the receptor N-terminus as a major binding domain for antagonists and agonists. Wille et al. showed that aa 43−50 and 76−84 represent crucial contact domains, which is supported also by work of Assil et al., who demonstrated the importance of Cys^{68}−Glu^{109} as a ligand binding domain. However, no individual amino acid interaction of the corresponding ligand has been described so far by these approaches. Besides the receptor N-terminus, it has also been shown that the extracellular loops may be involved in ligand binding. Perrin et al. (*14*) demonstrated with CRF/GRF receptor chimera that the extracellular receptor loops (EC2−EC4) contribute to binding. Liaw et al. (*19*) localized crucial binding determinants for sauvagine,

* Address correspondence to this author. Phone: +49(0)30-94793-240. Fax: +49(0)30-94793-159. E-mail: kraetke@fmp-berlin.de.

‡ Institute of Molecular Pharmacology.

§ Université de Sherbrooke.

[1] Abbreviations: aa, amino acid(s); Bpa, *p*-benzoyl-L-phenylalanine; BNPS-skatole, 2-(2′-nitrophenylsulfenyl)-3-methyl-3-bromoindolenine; CRF_1R, corticotropin-releasing factor receptor type 1; DMEM, Dulbecco's modified Eagle's medium, EC, extracellular domain; GPCR, G-protein-coupled receptor; GTPγS, guanosine 5′-*O*-(3-thiotriphosphate); HEK, human embryonic kidney; PNGase F, peptide *N*-glycosidase F; PTX, pertussis toxin; SDS−PAGE, sodium dodecyl sulfate−polyacrylamide gel electrophoresis; TM, transmembrane region; Ucn, urocortin.

10.1021/bi0507027 CCC: $30.25
Published on Web 11/03/2005

urocortin, and h/rCRF to aa 175−178 and 189, part of the first extracellular loop (EC2), and to aa 254 and 266−268, part of the second extracellular loop (EC3) of CRF_1R.

In summary, these results led to the assumption of a principle ligand binding orientation. It has been suggested that ligand binding at CRF_1R occurs by a "two-binding domain" orientation, in which the ligand C-terminus binds to the receptor N-terminus, representing the main binding domain, whereas the ligand N-terminus dips into the receptor juxtamembrane domain, provoking receptor activation (*20*−*22*). By NMR spectroscopic investigation of a soluble N-terminus of the $CRF_2\beta$ receptor alone and in complex with peptide ligands (astressin or oCRF), Grace et al. (*23*) obtained the first insights into the molecular basis of interaction. NMR data show that the soluble receptor N-terminus binds almost completely the antagonist astressin, which is, in contrast to peptide agonists, N-terminally truncated by about 10 aa, suggesting that the very N-terminus of agonists is oriented to the juxtamembrane region. Klose et al. (*24*) reported on the binding behavior of N-terminally truncated urocortins to soluble receptor N-termini. They proposed a three-domain binding model, in that the urocortin C-terminus (aa 32−40) and the N-terminal part (aa 1−21) are organized as two segregated binding domains. Moreover, the N-terminal domain (aa 1−21) also consists of two segregated sites; one is responsible for receptor activation (aa 1−11) and the other (aa 12−21) for ligand binding at the receptor N-terminus. After all, this extended model fits well to the fact of two different binding sites (aa 43−50 and aa 76−84) identified within the receptor N-terminus.

All of these reports identified crucial receptor binding determinants and led to the first models of ligand−receptor binding, but there is still no proof by a direct approach, i.e., direct determination of contact points between specific ligand amino acids and receptor domains. To address this question, the method of photoaffinity cross-linking has been applied. In principle, a selective radioactively labeled ligand is covalently cross-linked to its cognate receptor, and by chemical or enzymatic fragmentation of the complex, the ligand-bound domain of the receptor can be identified. This technique complements the limited conclusions of site-directed mutagenesis, deletion analysis, or chimeric receptors in that it not only is a more direct attempt to identify cross-linking sites within the receptor but also allows assignment of the corresponding ligand amino acids as well. This approach has been invaluable in mapping the ligand binding pocket of the β-adrenergic receptor (*25*), GnRH receptor (*26*), adenosine receptor (*27*), NK1-receptor (*28*), urotensin 2 receptor (*29*), angiotensin II receptor type 1 (*30*), and other members of class 1 GPCRs. In comparison, for class 2 GPCRs relatively little has been done so far. Photoaffinity cross-linking studies were carried out with corresponding Bpa-bearing ligands and the parathyroid hormone receptor (*31*, *32*), secretin receptor (*33*), calcitonin receptor (*34*), and vasoactive intestinal peptide receptor (*35*, *36*) (for review see ref *37*). In the case of CRF_1R, the only cross-linking study reported so far was done by Assil-Kishawi et al. (*38*). By use of a bifunctional chemical cross-linker, disuccinimidyl suberate (DSS), they identified position Lys^{16} of sauvagine interacting with Lys^{257} (EC3) of the CRF_1 receptor.

In contrast to the work of Assil-Kishawi et al., we applied the photoaffinity cross-linking approach to CRF receptors for the first time with the intention to prove the ligand−receptor interaction model derived from indirect approaches and to determine the orientation of the ligand N-terminus during binding that is responsible for receptor activation. We synthesized and characterized photoreactive analogues of rat urocortin substituted by *p*-benzoyl-L-phenylalanine (Bpa) in positions 0, 12, 17, or 22, which were applied to photolabeling of CRF_1 receptors stably expressed in HEK293 cells. Specific enzymatic and/or chemical fragmentations of the isolated, cross-linked ligand−receptor complex led to the identification of cross-linking sites within the receptor. Our findings of cross-linking sites located in the full-length receptor are in line with results obtained from investigations of possible receptor binding domains reported by others. However, we observed a different cross-linking site for urocortin than was described for sauvagine by use of the chemical cross-linking reagent DSS at a comparable position, suggesting that the two ligands bind with a different orientation or, alternatively, the difference is related to the limited properties of the cross-linking reagent DSS, which contains a large spacer between both chemoreactive groups. Furthermore, we also show that the mode of ligand binding deduced from systems expressing a soluble receptor N-terminus differs with our findings related to the full-length receptor.

EXPERIMENTAL PROCEDURES

Materials. All cell culture materials were supplied by Cotech (Berlin, Germany). Dulbecco's modified Eagle's medium (DMEM) was purchased from Biochrome (Berlin, Germany), and fetal calf serum was from PAN-SYSTEMS GmbH (Nürnberg, Germany). The HEK293 cell line, stably expressing the rat CRF_1 receptor, subcloned into the pcDNA3 vector, was kindly provided by Doreen Wietfeld (FMP-Berlin, Department of Peptide Chemistry). The radioligand ^{125}I-Y^0-sauvagine (2200 Ci/mmol) and the [γ-^{35}S]GTPγS (1250 Ci/mmol) were from PerkinElmer Life Sciences (Boston, MA). PNGase F was from New England Biolabs (Frankfurt am Main, Germany), and staphylococcal V8 (Glu-C) and Lys-C enzymes were purchased from Roche Diagnostics (Mannheim, Germany). The ^{125}I radionuclide, used for radioiodination procedures, was from PerkinElmer (Jügesheim, Germany). The photoreactive Y^0-Bpa-urocortin analogues were synthesized in our group by standard solid-phase peptide synthesis using N^{α}-Fmoc protection and a multiple peptide synthesizer excluding daylight as described previously (*39*). All peptides were synthesized with an additional tyrosine residue at the very N-terminus for radioiodination. After final cleavage with trifluoroacetic acid−10% water (v/v), the peptides were purified by preparative HPLC. All products were characterized by analytical HPLC (>95%), and mass spectrometric analysis (ESI-MS) gave the expected masses.

Peptide Labeling. Radioiodination of the Y^0-Bpa peptides was performed with the IODOGEN kit from Pierce Chemical Co. (Bonn, Germany) as described by Fraker and Speck (*40*). Briefly, 10 μL of a 1 mM peptide solution was incubated with 10 μL of $Na^{125}I$ radionuclide (1 mCi), 70 μL of distilled water, and 10 μL of 2 M acetic acid for 20 min in tubes precoated with IODOGEN followed by HPLC purification (Jasco HPLC-System, Germany) on a C_{18} column (10 mm × 250 mm, 5 μm particle size, 300 Å pore size). An eluent

gradient of 5−90% (v/v) acetonitrile/water (0.1% TFA) over 50 min with a flow rate of 1.0 mL/min was used.

The mean specific activity of the ^{125}I-Y^0-Bpa-Ucn analogues was estimated to be 150 Ci/mmol.

Cell Culture. HEK293 cells (previously obtained from the Deutsche Stammsammlung für Mikroorganismen und Zellkulturen), stably transfected with the pcDNA3 vector encoding for CRF_1R (average B_{max} of 8×10^{-11} mol/mg of protein), were a gift of Doreen Wietfeld (FMP-Berlin). The cells were maintained in DMEM supplemented with 10% fetal calf serum, 5 mL of L-glutamine, 100 units/mL penicillin G, 100 μg/mL streptomycin sulfate, and 400 μg/mL G418 sulfate (Geniticin) at 37 °C in a humidified atmosphere of 90% air and 10% CO_2. For photoaffinity cross-linking experiments, cells were cultivated on 100 mm culture dishes until they reached confluence before they were washed with PBS and stored at −80 °C.

Receptor Displacement Assay Performed with CRF_1R HEK Cell Membranes. Cell membranes were prepared as described previously by Wietfeld et al. (*41*). Membrane protein (1.25 μg) in 300 μL of assay buffer [50 mM Tris-HCl (pH 7.2), 0.15 mM bacitracin, 0.0015% aprotinin, 10 mM $MgCl_2$, 2 mM EGTA, 0.1% BSA] was incubated in triplicate with 0.1 nM ^{125}I-Y^0-sauvagine in the absence and presence of six different concentrations (10^{-6} to 10^{-12} M) of unlabeled Y^0-Bpa-Ucn analogues at 25 °C for 2 h. The samples were then immediately filtered through GF/C filter disks (Whatman), presoaked for 2 h in 0.1% poly(ethylenimine), using a Brandel harvester. The incubation tubes and filters were washed three times with 3 mL of cold washing buffer (50 mM Tris-HCl, 10 mM $MgCl_2$, 2 mM EGTA, 0.01% Triton X-100, pH 7.2). Triton X-100 in this buffer strongly reduced nonspecific tracer binding. Radioactivity retained on the filter was measured by γ-counting (counter efficiency was about 70%). Receptor affinities were calculated using the nonlinear least-squares curve-fitting program RADLIG from Biosoft (Cambridge, U.K.).

Receptor/G-Protein Coupling of Bpa Peptides Estimated by Binding of [γ-^{35}S]GTPγS to CRF_1R HEK Cell Membranes. The biological activity of the CRF_1R ligands was measured by their stimulation of [γ-^{35}S]GTPγS binding in CRF_1R cell membranes as described earlier by Wietfeld et al. (*41*). Briefly, about 5 μg of cell membranes exhibiting CRF_1R-stimulated G_s or G_i activity were incubated in triplicate at 25 °C with 125 pM [γ-^{35}S]GTPγS in a medium consisting of 50 mM Tris-HCl (pH 7.4), 100 mM NaCl, 0.1 μM GDP, 10 mM $MgCl_2$, 0.2 mM EGTA, 1 mg/mL BSA, and 0.15 mM bacitracin for 2 h. The reaction was terminated by filtration through Whatman GF/B filters using a Brandel harvester (Gaithersburg, MD). Concentration−response curves for the stimulation of [^{35}S]GTPγS binding by sauvagine, urocortin, Y^{-1}-Bpa^0-Ucn, Y^0-Bpa^{12}-Ucn, Y^0-Bpa^{17}-Ucn, and Y^0-Bpa^{22}-Ucn were fitted by nonlinear regression using the program PRISM 4 (GraphPad Software, San Diego, CA).

Photoaffinity Cross-Linking of HEK-CRF_1R Cells with ^{125}I-Y^0-Bpa Peptides. Photoaffinity cross-linking was performed as described previously by Boucard et al. (*30*). Stably transfected HEK293 cells, expressing the CRF_1 receptor, were incubated at room temperature for 90 min in the dark in 0.5 mL of binding buffer [20 mM Tris-HCl (pH 7.8), 5 mM $MgCl_2$, 0.1% BSA (w/v)] containing the photoreactive ligand (2.4×10^7 cpm, average specific activity of 150 Ci/mmol)). The cells were then centrifuged (3000*g*, 10 min, room temperature), resuspended in 0.5 mL of binding buffer, and irradiated for 60 min on ice under filtered UV light (λ = 365 nm, five lamps at 15 W). After irradiation, the cell suspension was centrifuged (3400*g*, 10 min, 4 °C) and resuspended in modified solubilization buffer [50 mM Tris-HCl (pH 7.4), 150 mM NaCl, 1% Nonidet P-40, 0.1% sodium deoxycholate] for 45−60 min on ice. After centrifugation (13000*g*, 15 min, 4 °C), the supernatant was divided into portions and kept at −80 °C until further analysis.

For determination of the cross-linking efficiency two samples with equivalent amount of cells (1×10^6 cells each), stably expressing the CRF_1 receptor, were incubated in binding buffer in the presence and absence of 10^{-7} M Y^0-Bpa^{22}-Ucn for 90 min at room temperature in the dark before they were irradiated with UV light (λ = 365 nm, five lamps at 15 W) on ice for 60 min. The cells were then harvested (3400*g*, 15 min, 4 °C) and washed twice with binding buffer before they were used in a receptor displacement assay for the determination of the cross-linking efficiency.

Partial Purification of the Cross-Linked Ligand−Receptor Complex. Ligand−receptor conjugates were partially purified as previously described by Boucard et al. (*30*). The cross-linked ligand−receptor complex was separated by SDS−PAGE on 10% acrylamide Tris−glycine gels according to the method of Laemmli (*42*) before being exposed to X-ray films (Hyperfilm MP, Amersham). The band corresponding to the ligand−receptor complex was cut out from the gel, transferred into a dialysis chamber, and submitted to an electroelution step using SDS−PAGE running buffer. The eluted ligand−receptor complex was then concentrated with Vivaspin centrifugal filters (VWR International, Germany) and kept at −80 °C until further analysis.

Endoglycosidase, Enzymatic, and Chemical Cleavages. The cleavage procedures were performed with partially purified ligand−receptor conjugates (5000−30000 cpm). For deglycosylation, the conjugate was diluted with deglycosylation buffer [150 mM Tris-HCl (pH 7.4), 50 mM EDTA, 1% 2-mercaptoethanol], PNGase F (500 units) was added, and samples were incubated at 37 °C for 16−20 h.

For CNBr cleavage, the conjugate was diluted in a final mixture of 70% formic acid containing 100 mg/mL CNBr and incubated in the dark for 24−48 h at room temperature.

BNPS-skatole-mediated cleavage of the conjugate was performed in a final mixture of 60% acetic acid and 25% BNPS-skatole (2 mg/mL) for 24−48 h at room temperature in the dark.

Glu-C and Lys-C cleavages of the conjugates were performed with 1 and 0.5 μg of enzyme, respectively, in 25 mM ammonium bicarbonate for 48−72 h at room temperature in the dark.

All reactions were terminated by adding 1 mL of water to the samples followed by freeze-drying.

Analysis of Products Obtained by Chemical and Enzymatic Cleavage. The products of cleavage and deglycosylation were analyzed by SDS−PAGE using high-resolution 16.5% acrylamide Tris−Tricine gels followed by autoradiography on X-ray films (Hyperfilm MP, Amersham) including intensifying screens (Amersham). A ^{14}C-labeled low-molec-

Table 1: Receptor Binding Affinities and Potencies for G-Protein Stimulation of Y^0-Bpa Peptides in HEK-CRF_1R Cell Membranes[a]

ligand	$K_i \pm$ SEM (M) (receptor binding)	$EC_{50} \pm$ SEM (M) (G_s potency)	$EC_{50} \pm$ SEM (M) (G_i potency)
sauvagine	$8.34 \times 10^{-10} \pm 4.03 \times 10^{-11}$	$3.31 \times 10^{-11} \pm 5.26 \times 10^{-12}$	$2.50 \times 10^{-9} \pm 8.59 \times 10^{10}$
urocortin	$1.77 \times 10^{-10} \pm 1.03 \times 10^{-11}$	$1.20 \times 10^{-11} \pm 2.11 \times 10^{-12}$	$4.56 \times 10^{-10} \pm 2.23 \times 10^{-11}$
Tyr^{-1}-Bpa^0-Ucn	$2.87 \times 10^{-10} \pm 3.89 \times 10^{-11}$	$7.15 \times 10^{-11} \pm 6.70 \times 10^{-12}$	$1.12 \times 10^{-9} \pm 1.01 \times 10^{-10}$
Tyr^0-Bpa^{12}-Ucn	$4.02 \times 10^{-10} \pm 4.04 \times 10^{-11}$	$1.97 \times 10^{-10} \pm 3.44 \times 10^{-11}$	$6.35 \times 10^{-9} \pm 1.07 \times 10^{-9}$
Tyr^0-Bpa^{17}-Ucn	$2.84 \times 10^{-10} \pm 2.45 \times 10^{-11}$	$5.06 \times 10^{-11} \pm 5.81 \times 10^{-12}$	$8.56 \times 10^{-10} \pm 2.73 \times 10^{-10}$
Tyr^0-Bpa^{22}-Ucn	$2.00 \times 10^{-10} \pm 7.19 \times 10^{-12}$	$5.53 \times 10^{-11} \pm 7.16 \times 10^{-12}$	$1.83 \times 10^{-9} \pm 3.68 \times 10^{-10}$

[a] The table shows estimated K_i values, determined by displacement assays, and the G_s and G_i activity, determined by [γ-^{35}S]GTPγS assays, which are presented as the mean $\pm$ SEM of at least three independent experiments performed on membranes obtained from HEK cells stably expressing the CRF_1 receptor. Bpa = *p*-benzoyl-L-phenylalanine.

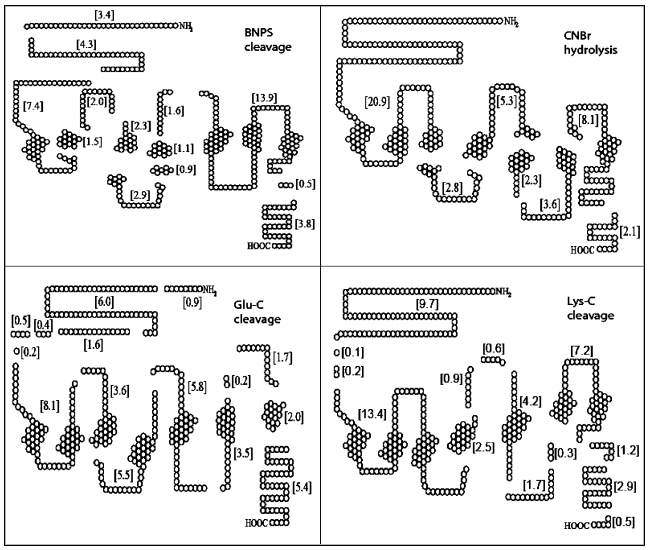

FIGURE 1: Theoretical CRF_1R fragmentation pattern. The figure shows the theoretical fragmentation fingerprint of the $rCRF_1$ receptor in dependency on the cleavage performed. The molecular mass of fragments is indicated by numbers in square brackets (kDa). The cleaved signal sequence (aa 1−23) and the N-terminal glycosylation sites are not shown in the figure.

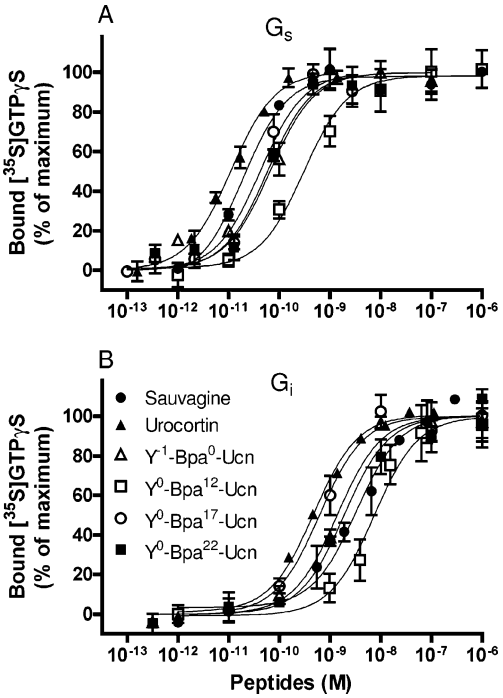

FIGURE 2: Concentration−response curves for the stimulation of [γ-^{35}S]GTPγS binding by sauvagine, urocortin, and Y^0-Bpa-Ucn analogues to HEK-CRF_1R cell membranes. To observe selectively G_s- (A) and G_i-coupled activity (B), cell membranes were obtained from HEK-CRF_1R cells pretreated with 100 ng/mL PTX for 24 h and with 0.1 μM sauvagine for 4 h, respectively, as found recently (*41*). Data points are normalized with the basal and maximum response taken at 0 and 100%, respectively. Data are represented as the mean $\pm$ SD from triplicates.

ular-mass protein standard (Amersham) was used to determine the apparent molecular masses.

RESULTS

Receptor Binding of Photoreactive Ligands. Table 1 shows the K_i values of sauvagine, urocortin, and all Y^0-Bpa analogues used in the present study, determined by displacement assays using ^{125}I-Y^0-sauvagine as tracer. The binding constants found for the photoreactive analogues are comparable to urocortin and sauvagine and therefore proved high-affinity binding. All values are representative of at least three independent assays and are given as the mean $\pm$ SEM.

Bpa Peptides Evoked CRF_1R/G-Protein Coupling Estimated by Stimulation of the Binding of [γ-^{35}S]GTPγS to CRF_1R Cell Membranes. Figure 2 shows the results of a [γ-^{35}S]GTPγS assay performed with Y^{-1}-Bpa^0-Ucn, Y^0-Bpa^{12}-Ucn, Y^0-Bpa^{17}-Ucn, Y^0-Bpa^{22}-Ucn, sauvagine, and urocortin. The estimated EC_{50} values are summarized in Table 1. The intrinsic activities for the G_s and G_i activation of urocortin and the corresponding Y^0-Bpa^x-urocortins were found to be in the range of 96.84−109.64% as compared to sauvagine (not significantly different). It is therefore concluded that all photoreactive peptides used here are full G-protein-activating high-potency agonists at the CRF_1R.

Efficiency of Cross-Linking and Characterization of the Cross-Linked Ligand−Receptor Complex. Table 2 summarizes the results of a cross-linking experiment used for the calculation of the cross-linking efficiency, which was obtained by a displacement assay using the Y^0-Bpa^{22}-Ucn analogue as a representative cross-linking analogue and ^{125}I-Y^0-sauvagine as tracer (see Experimental Procedures). Comparison of B_{max} values of the irradiated sample containing binding buffer only and the sample containing the Y^0-Bpa^{22}-Ucn analogue resulted in a cross-linking efficiency of about 50%.

Further characterization of photoaffinity cross-linking by SDS−PAGE gels displayed a glycosylated ligand−receptor complex migrating at an apparent mass of 80 kDa (Figure 3A), which was specifically and covalently cross-linked by use of each of the^{125}I-Y^0-Bpa peptides and corresponds to the calculated mass. (The predominant band visible at 29 kDa is a result of the migration front due to the stop of the gel at this point and contains remaining free ligand. It does not represent a peptide migrating naturally at the observed mass.)

Table 2: Characterization of the Cross-Linking Efficiency of Y^0-Bpa^{22}-Ucn to HEK-CRF_1R Cell Membranes[a]

treatment	$K_d \pm$ SD (M)	$B_{max} \pm$ SD (mol/mg)
irradiated only	$2.78 \times 10^{-10} \pm 9.36 \times 10^{-11}$	$5.78 \times 10^{-11} \pm 5.93 \times 10^{-12}$
10^{-7} M Y^0-Bpa^{22}-Ucn, irradiated	$7.36 \times 10^{-10} \pm 1.24 \times 10^{-10}$	$2.99 \times 10^{-11} \pm 1.19 \times 10^{-12}$

[a] The table shows estimated B_{max} values of a cross-linking experiment performed with a displacement assay on HEK-CRF_1R cell membranes using ^{125}I-Y^0-sauvagine as tracer and the Y^0-Bpa^{22}-Ucn analogue as a representative cross-linking analogue. According to the estimated B_{max} values, which are given as the mean $\pm$ SD, a cross-linking efficiency of about 50% was calculated for the Bpa peptide.

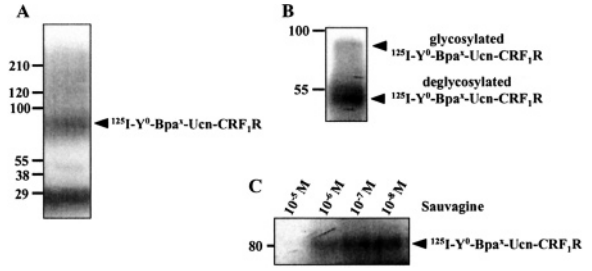

FIGURE 3: Photoaffinity cross-linking and characterization of the ligand−receptor complex. The figure shows representative gel pictures from 10% Tris−glycine gels used to separate cross-linked ^{125}I-Y^0-Bpa-Ucn ligand−receptor complexes followed by autoradiography. Molecular masses are indicated (kDa). (A) Shown is a representative glycosylated ligand−receptor complex migrating at approximately 80 kDa. (B) Deglycosylation of the partially purified ligand−receptor complex with PNGase F shifted the band to approximately 50 kDa, indicating its nonglycosylated nature. (C) Specificity of the cross-linking step was checked in the presence of increasing concentrations of unlabeled sauvagine, showing a complete abolition of cross-linking.

Deglycosylation with PNGase F reduced the size of the ligand−receptor complex to approximately 50 kDa (Figure 3B). Confirmation of the cross-linking specificity was proven by incubation of the ^{125}I-Y^0-Bpa^x peptide and the receptor in the presence of increasing concentrations of unlabeled sauvagine, which led to abolition of the cross-linking step (Figure 3C).

Peptide Mapping of the ^{125}I-Y^{-1}-Bpa^0-Urocortin Receptor Complex. (A) BNPS-Skatole Cleavage. For peptide mapping of the cross-linked ^{125}I-Y^{-1}-Bpa^0-Ucn receptor complex an initial mapping step was performed by BNPS-skatole, which cleaves C-terminally of tryptophan residues. The cleavage produced a broad band with an apparent molecular mass of about 20 kDa (Figure 4A). Deglycosylation of the ligand−receptor fragment with PNGase F did not alter the migration pattern, indicating its nonglycosylated nature. The band should theoretically be composed of the 5 kDa ligand and a receptor fragment of approximately 15 kDa. Due to the nonglycosylated nature and the size observed, the potential receptor fragment is represented by the second (EC3) and third (EC4) extracellular loops connected by TM5−7 (13.9 kDa), spanning the residues from Phe^{260} to Trp^{378}. The calculated mass of this possible ligand−receptor complex fragment (18.9 kDa) is close to the observed one (20 kDa; see fragmentation pattern in Figure 1).

(B) CNBr Cleavage. For a more detailed localization of the cross-linking site, the ligand−receptor conjugate was subjected to CNBr, which cleaves C-terminally of methionine residues. CNBr cleavage of glycosylated or deglycosylated conjugates in both cases produced a single band migrating at approximately 10 kDa, indicating that the cross-linking product obtained was nonglycosylated. It should be composed of the 5 kDa ligand and a receptor fragment of approximately 5 kDa (Figure 4B). The potential receptor fragment refers to the second extracellular loop (EC3) elongated by parts of TM4 and TM5 (5.3 kDa), spanning the residues from Phe^{231} to Met^{276}. The observed apparent mass (10 kDa) fits very well to the calculated one (10.3 kDa).

(C) Glu-C Cleavage. To validate the results from BNPS-skatole and CNBr degradations, partially purified ligand−receptor complex was subjected to Glu-C, which cleaves C-terminally of glutamic acid residues. It is noteworthy that Glu-C also cleaves the ligand (between positions 19 and 20), generating a ligand fragment of about 2.5 kDa (^{125}I-Y^{-1}-Bpa^0-Ucn^{1-19}). The enzymatic cleavage resulted in a broad band with an apparent mass of about 8 kDa (Figure 4C). It should be consisted of the 2.5 kDa ligand fragment and a receptor fragment of approximately 5.5 kDa. The observed receptor fragment was assigned to represent a part of the second extracellular loop (EC3) including TM5 (5.8 kDa), spanning receptor residues from Lys^{257} to Glu^{305}, plus the cleaved ligand (2.5 kDa). The calculated mass (8.3 kDa) refers to the apparent mass observed (8 kDa).

Taken into consideration the three cleavage patterns obtained, the minimal domain of the cross-linked receptor for the ^{125}I-Y^{-1}-Bpa^0-Ucn analogue can be pinned down to the second extracellular loop (EC3) of CRF_1R, spanning the residues from Phe^{260} to Met^{276}.

Peptide Mapping of the ^{125}I-Y^0-Bpa^{12}-Urocortin Receptor Complex. Degradation of the ^{125}I-Y^0-Bpa^{12}-Ucn receptor complex using BNPS-skatole, CNBr, and Glu-C resulted in a cleavage pattern equivalent to that obtained for the ^{125}I-Y^{-1}-Bpa^0-Ucn receptor complex. Therefore, the pictures shown in Figure 4 are representative for this analogue as well. In summary, ^{125}I-Y^{-1}-Bpa^0-Ucn and ^{125}I-Y^0-Bpa^{12}-Ucn share the same cross-linking domain within CRF_1R, which is located in the second extracellular loop (EC3) spanning the residues from Phe^{260} to Met^{276}.

Peptide Mapping of the ^{125}I-Y^0-Bpa^{17}-Urocortin Receptor Complex. (A) CNBr Cleavage. The cross-linked ^{125}I-Y^0-Bpa^{17}-Ucn receptor complex was deglycosylated and subjected to CNBr cleavage, resulting in a single band migrating at a molecular mass of approximately 28 kDa (Figure 5A). Theoretically, the observed fragment should be composed of the 5 kDa ligand and a 23 kDa receptor fragment. According to the possible fragmentation pattern (see Figure 1), the observed receptor fragment was assigned to be composed of the N-terminus (EC1) including the first extracellular loop (EC2) elongated by TM1−3 (20.9 kDa). The small deviation between the calculated (20.9 kDa) and observed (23 kDa) receptor fragment is presumably accounted for by an incomplete deglycosylation or cleavage. It can be excluded that any other fragment refers to the observed mass upon CNBr cleavage because no other fragment theoretically fits to the observed size.

(B) BNPS-Skatole Cleavage. For further restriction of the cross-linking site, partially purified glycosylated and deg-

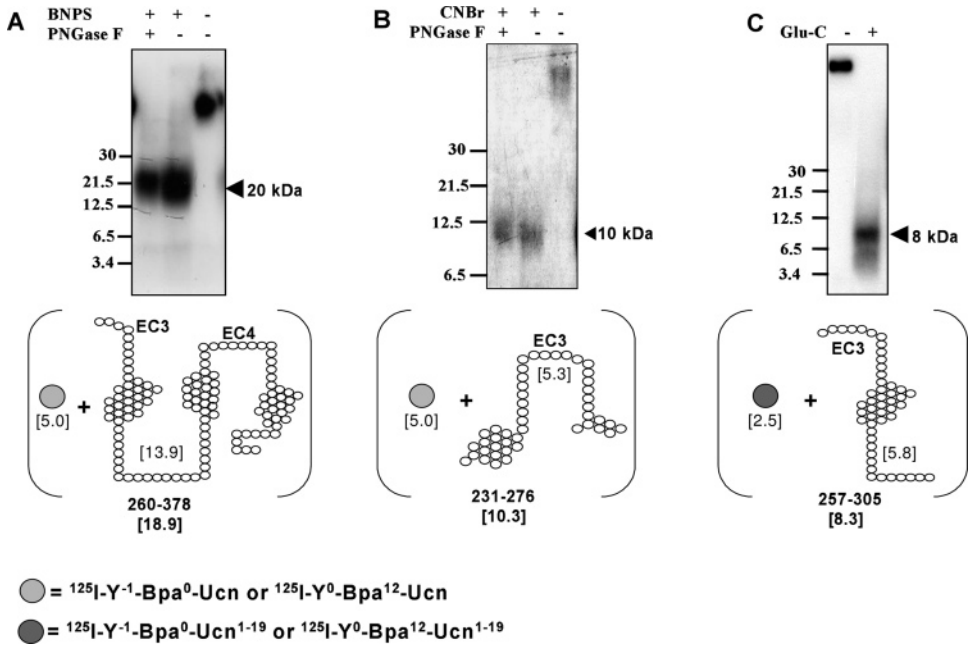

FIGURE 4: Peptide mapping of the ^{125}I-Y^{-1}-Bpa^{0}-Ucn and ^{125}I-Y^{0}-Bpa^{12}-Ucn receptor complex. Shown are representative pictures from 16.5% acrylamide Tris−Tricine gels used to separate the cleaved products of the ^{125}I-Y^{-1}Bpa^{0}-Ucn and ^{125}I-Y^{0}-Bpa^{12}-Ucn receptor complex, followed by autoradiography. Molecular mass markers are indicated (kDa). Since both peptides showed equivalent cleavage patterns, they are summarized together in the figure. Below each picture a schematic representation of the ligand and the identified and allocated receptor fragment is shown. The numbers in square brackets indicate the molecular mass of the identified fragment. The receptor-allocated residues are shown in bold numbers at the very bottom, while the total mass of the calculated ligand−receptor fragment is highlighted by bold numbers in brackets. (A) Incubation of the partially purified glycosylated and deglycosylated ligand−receptor complex with BNPS in both cases resulted in a band with an apparent mass of about 20 kDa. The band was assigned to be a cross-linking product composed of the ligand (5 kDa) and the receptor fragment from Phe^{260} to Trp^{378} (13.9 kDa). The treatment with PNGase F proved the nonglycosylated nature of the observed fragment. (B) CNBr cleavage of the glycosylated and deglycosylated ligand−receptor complex in both cases displayed a weak band migrating at approximately 10 kDa and was allocated to the receptor fragment from Phe^{231} to Met^{276} (5.3 kDa) and the ligand (5 kDa). (C) Cleavage with Glu-C led to a band migrating with an apparent mass of about 8 kDa and was assigned to the ligand fragment ^{125}I-Y^{-1}-Bpa^{0}-Ucn$^{1-19}$ or ^{125}I-Y^{0}-Bpa^{12}-Ucn$^{1-19}$ (2.5 kDa) and the receptor fragment from Lys^{257} to Glu^{305} (5.8 kDa).

lycosylated conjugates were digested with BNPS-skatole, providing a weak band with an apparent mass of about 7.5 kDa in both cases (Figure 5B). In principle, the observed fragment should correspond to a 2.5 kDa receptor fragment cross-linked to the ligand (5 kDa). The receptor fragment was assigned to represent EC2, spanning the residues from Phe^{170} to Trp^{187} (2.0 kDa) plus the cross-linked ligand (5 kDa). The observed apparent mass (7.5 kDa) is very close to the calculated mass (7 kDa). The nonglycosylated nature of the observed fragment also supports the assignment.

(C) Lys-C Cleavage. To confirm the allocated cross-linking site of the affinity label, the partially purified ligand−receptor complex was subjected to PNGase F followed by Lys-C cleavage, which resulted in a weak band with an apparent molecular mass of approximately 19 kDa (Figure 5C). This band should be composed of the 5 kDa ligand and a 14 kDa receptor fragment. Considering the already localized cross-linking site, the receptor fragment corresponds to EC1-TM1-TM2-EC2-TM3 (13.4 kDa), spanning the residues from Val^{114} to Lys^{228} plus the ligand. The observed mass (19 kDa) is in agreement with the calculated one (18.4 kDa).

(D) Glu-C Cleavage. Deglycosylation of the ligand−receptor complex followed by Glu-C cleavage led to a band with an apparent molecular mass of 10 kDa (Figure 5D). The observed band should be composed of the 2.5 kDa ligand fragment (cleaved after Glu^{19}) and a 7.5 kDa receptor fragment. The observed fragment was assigned to a complex composed of ^{125}I-Y^{0}-Bpa^{17}-Ucn$^{1-19}$ (2.5 kDa) and the receptor fragment EC1-TM1-TM2-EC2 (8.1 kDa), spanning the receptor residues from Lys^{110} to Glu^{179}. The calculated mass (10.6 kDa) is very close to the observed mass (10 kDa).

Considering all obtained cleavage patterns, the minimal cross-linking domain for Bpa at position 17 can be restricted to the first extracellular loop (EC2) of CRF$_1$R, spanning the residues from Trp^{170} to Glu^{179}.

Peptide Mapping of the ^{125}I-Y^{0}-Bpa^{22}-Urocortin Receptor Complex. In the case of the ^{125}I-Y^{0}-Bpa^{22}-Ucn receptor complex equivalent cleavage patterns were observed as for the ^{125}I-Y^{0}-Bpa^{17}-Ucn analogue by use of BNPS, CNBr, and Lys-C. Therefore, a common cross-linking domain exists for Bpa at positions 17 and 22, which is located at the first extracellular loop (EC2) of CRF$_1$R (see Figure 5) spanning the residues from Trp^{170} to Glu^{179}.

DISCUSSION

For identifying the molecular basis of ligand−receptor interaction, it is of importance to understand the initial binding steps leading to receptor activation. Investigations using indirect approaches such as chimeric receptors, deletion mutants, and amino acid replacements have led to elucidation of important ligand binding determinants of CRF receptors and development of the first models, such as the two-binding domain model and the receptor N-terminus as the main ligand binding site (*20*−*22*). However, there is no direct information on contact points between CRF receptors and specific ligand amino acids so far. In the present study the method of

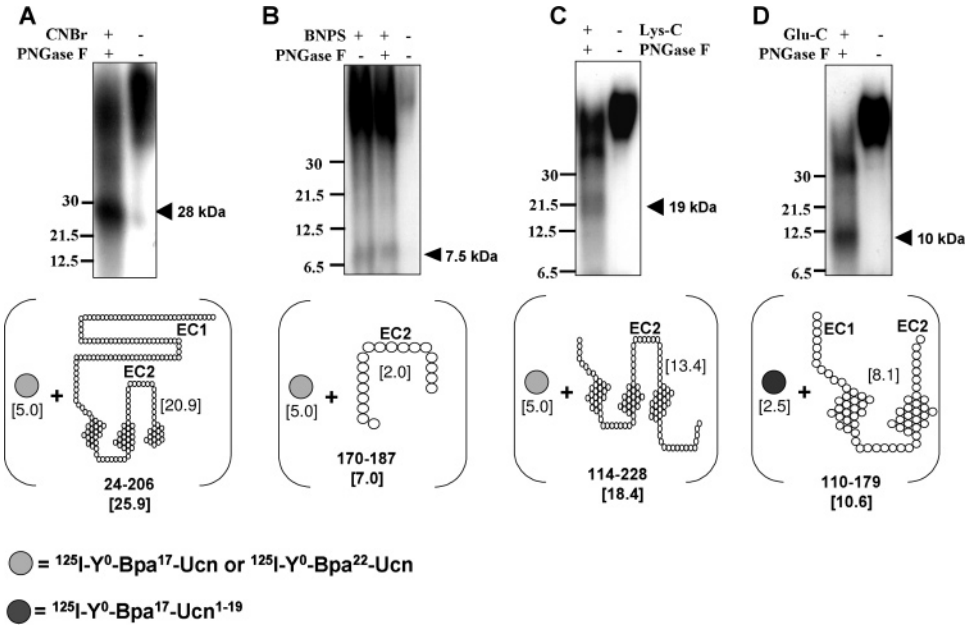

FIGURE 5: Peptide mapping of the ^{125}I-Y^0-Bpa^{17}-Ucn and ^{125}I-Y^0-Bpa^{22}-Ucn receptor complex. Shown are representative gel pictures of the ^{125}I-Y^0-Bpa^{17}-Ucn and ^{125}I-Y^0-Bpa^{22}-Ucn receptor complex after different cleavage methods, separated on 16.5% acrylamide Tris−Tricine gels followed by autoradiography. Because both analogues share the same cross-linking site, derived by equivalent cleavage patterns, they are summarized together. Molecular mass markers are indicated (kDa). Below, schematic representations of the ligand and assigned receptor fragment are shown. The numbers in square brackets indicate the molecular mass of the identified fragment. The identified receptor-allocated residues are shown in bold numbers at the very bottom, while the total mass of the calculated ligand−receptor fragment is highlighted by bold numbers in brackets. (A) Shown is the result of a deglycosylation with PNGase F followed by CNBr cleavage, which resulted in a band migrating at approximately 28 kDa. The band was assigned to the receptor fragment from Ser^{24} to Met^{206} (20.9 kDa) and the cross-linked ligand (5 kDa). (B) BNPS-skatole cleavage of glycosylated and deglycosylated conjugate showed a weak band with an apparent mass of about 7.5 kDa. The observed band was assigned to represent the receptor fragment from Phe^{170} to Trp^{187} (2.0 kDa) cross-linked to the ligand (5 kDa). (C) Deglycosylation of the conjugate followed by Lys-C cleavage created a band migrating at approximately 19 kDa and was assigned to the receptor fragment from Val^{114} to Lys^{228} (13.4 kDa) and the ligand (5 kDa). (D) Deglycosylation of the ligand−receptor complex followed by Glu-C cleavage generated a ligand−receptor fragment with an apparent mass of 10 kDa and was referred to the receptor fragment from Lys^{110} to Glu^{179} (8.1 kDa) and the cleaved ligand ^{125}I-Y^0-Bpa^{17}-Ucn$^{1-19}$. A Glu-C cleavage of the ^{125}I-Y^0-Bpa^{22}-Ucn was not performed.

photoaffinity cross-linking was used to identify such contact domains between Bpa residues at different positions of urocortin and the CRF_1 receptor. This approach is strongly dependent on the spatial proximity between the photoreactive ligand group and receptor domains to form covalently bound ligand−receptor complexes, which can be subsequently and specifically cleaved to identify corresponding interaction sites.

At first, analogues of urocortin substituted with Bpa at positions 0, 12, 17, or 22 were chosen from a Bpa scan of urocortin (scan will be published elsewhere). Their high-affinity binding to CRF_1R was verified by displacement experiments (Table 1), and furthermore, [γ-^{35}S]GTPγS assays showed their high potencies (Table 1, Figure 2) and proved the full agonistic behavior of all analogues (see Results).

In photoaffinity cross-linking experiments the specificity of cross-linking was verified by a decreasing cross-linking yield in the presence of increasing concentrations of unlabeled sauvagine when one of the ^{125}I-Y^0-Bpa-Ucn analogues was incubated with receptors (Figure 3C). The average cross-linking efficiency was calculated to be 50% (Table 2). The ^{125}I-Y^0-Bpa-Ucn analogues specifically cross-linked to the CRF_1 receptor migrating as a ligand−receptor complex with an average mass of approximately 80 kDa in SDS−PAGE gels (Figure 3A). The susceptibility of the 80 kDa ligand−receptor complex to deglycosylation with PNGase F (Figure 3B) confirmed the glycosylated nature of the receptor as reported earlier (*43*, *44*).

Cleavages of ^{125}I-Y^0-Bpa-Ucn ligand−receptor complexes with Bpa at positions 0, 12, 17, or 22 led to a clear identification of distinct interacting sites located at extracellular receptor domains (EC). We show that residues 0 and 12 (^{125}I-Y^{-1}-Bpa^0-Ucn and ^{125}I-Y^0-Bpa^{12}-Ucn analogues) cross-linked to residues located within the second extracellular receptor loop (EC3), spanning the residues from Phe^{260} to Met^{276} (Figure 4). Results obtained for the two peptides are in line with findings of Liaw et al. (*19*), who suggested a ligand binding site between Val^{266} and Thr^{268} as derived from receptor mutagenesis studies. Furthermore, residues 17 and 22 (^{125}I-Y^0-Bpa^{17}-Ucn and ^{125}I-Bpa^{22}-Ucn analogues) were found to cross-link to the first extracellular receptor loop (EC2), spanning the residues from Trp^{170} to Glu^{179} of the receptor (Figure 5). Results of receptor mutagenesis studies (*19*) have correspondingly shown that the receptor residues 175−178 are likely to represent an important contact domain. Interestingly, Assil-Kishawi et al. (*38*) showed, using the bifunctional chemical cross-linker disuccinimidyl suberate (DSS), that position Lys^{16} in sauvagine cross-linked to Lys^{257} (EC3) of CRF_1R instead to EC2, which we identified as the cross-linking site for the Bpa^{17} in urocortin. This different result may be attributed to the fact that DSS cross-links ϵ-amino groups only and may be more flexible due to the suberate spacer than a benzophenone-substituted analogue, which represents only an elongation of the Phe side chain by one C atom. Otherwise, different cross-linking sites might simply be a result related to the fact that urocortin and

sauvagine seem to bind to different receptor domains as very recently concluded from receptor mutagenesis studies (*45*).

The fact that soluble receptor N-termini exhibited remarkable affinity to urocortin, in displacement assays using astressin as radioligand, suggested that the peptide ligand C-terminus binds almost completely to the receptor N-terminus, whereas the ligand N-terminus (≈10 aa) dips into the receptor juxtamembrane region, initiating receptor activation (*7*, *20*, *23*, *24*). This model is supported by the results of Klose et al. (*24*), who reported that N-terminal truncation of urocortin by up to 10 aa did not significantly affect the binding affinity to the soluble receptor N-terminus, whereas further truncations led to a complete loss in binding, suggesting that those residues (aa 11−40) bind to the soluble receptor N-terminus. On the contrary, the results of our photoaffinity cross-linking study show that aa at positions 12, 17, and 22 of urocortin bind to the juxtamembrane region of the full-length receptor and not to the receptor N-terminus. Although we did not locate contact domains between urocortin and the receptor N-terminus, our findings are not conflicting to the idea of the receptor N-terminus to be regarded as the dominant binding site for peptide ligands. It can be speculated that residues 12, 17, and 22 interact with the juxtamembrane region located on one side of the probably helical ligand molecule, whereas residues in between could be located at the opposite site interacting with the receptor N-terminus. Nevertheless, our findings indicate that there are differences between ligand binding of urocortin to a soluble receptor N-terminus and to the full-length receptor, a fact which makes it questionable to draw a general conclusion just from one system. Moreover, the question arises whether a soluble receptor N-terminus can be used as a representative tool for setting up a model of ligand binding interaction. In any case, the cross-linking sites identified in the present study underline the role of the receptor juxtamembrane for urocortin−CRF_1R binding, in that it arranges those N-terminal urocortin residues that are crucial for receptor activation in the right position.

Although other members of class 2 GPCRs, like PTH receptor (*31*, *32*, *46*, *47*), secretin receptor (*48*−*50*), and calcitonin receptor (*34*, *51*), have been examined by photoaffinity cross-linking studies with corresponding Bpa analogues, no common interaction mode can be recognized at the moment. Probably there exists a number of different interaction modes as indicated by mutagenesis studies of CRF_1 and CRF_2 receptors that bind natural ligands in a different manner (*45*). In ongoing studies we will extend our studies to elucidate interaction sites between urocortin analogues modified with Bpa in the C-terminal part and CRF receptors.

ACKNOWLEDGMENT

We thank D. Krause (FMP), A. Klose (FMP), B. Schmikale (FMP), G. Vogelreiter (FMP), M. Georgi (FMP), and M. R. Lefebvre (IPS) for excellent technical assistance in the field of peptide chemistry, M. Clement (IPS) for technical support and valuable hints, and D. Wietfeld (FMP) for supplying us with stably transfected HEK293 cells, encoding for CRF_1R. Dr. K. Fechner (FMP) is thanked for helpful support using the RADLIG software.

REFERENCES

1. Vaughan, J., Donaldson, C., Bittencourt, J., Perrin, M. H., Lewis, K., Sutton, S., Chan, R., Turnbull, A. V., Lovejoy, D., Rivier, C., and Rivier, D. (1995) Urocortin, a mammalian neuropeptide related to fish urotensin I and to corticotropin-releasing factor, *Nature 378*, 287−292.
2. Latchman, D. S. (2002) Urocortin, *Int. J. Biochem. Cell Biol. 34*, 907−910.
3. Zorrilla, E. P., Schulteis, G., Ormsby, A., Klaassen, A., Ling, N., McCarthy, J. R., Koob, G. F., and De Souza, E. B. (2002) Urocortin shares the memory modulating effects of corticotropin-releasing factor (CRF): mediation by CRF1 receptors, *Brain Res. 952*, 200−210.
4. De Souza, E. B. (1995) Corticotropin-releasing factor receptors: physiology, pharmacology, biochemistry and role in central nervous system and immune disorders, *Psychoneuroendocrinology 20*, 789−819.
5. Dieterich, K. D., Lehnert, H., and De Souza, E. B. (1997) Corticotropin-releasing factor receptors: an overview, *Exp. Clin. Endocrinol. Diabetes 105*, 65−82.
6. Owens, M. J., and Nemeroff, C. B. (1991) Physiology and pharmacology of corticotropin-releasing factor, *Pharmacol. Rev. 43*, 425−473.
7. Grigoriadis, D. E., Haddach, M., Ling, N., and Saunders, J. (2001) The CRF receptor: Structure, function and potential for therapeutic intervention, *Curr. Med. Chem.: Cent. Nerv. Syst. Agents 1*, 63−97.
8. Hauger, R. L., Grigoriadis, D. E., Dallman, M. F., Plotsky, P. M., Vale, W. W., and Dautzenberg, F. M. (2003) International Union of Pharmacology. XXXVI. Current status of the nomenclature for receptors for corticotropin-releasing factor and their ligands, *Pharmacol. Rev. 55*, 21−26.
9. Hillhouse, E. W., Randeva, H., Ladds, G., and Grammatopoulos, D. (2002) Corticotropin-releasing hormone receptors, *Biochem. Soc. Trans. 30*, 428−432.
10. Arai, M., Assil, I. Q., and Abou-Samra, A. B. (2001) Characterization of three corticotropin-releasing factor receptors in catfish: a novel third receptor is predominantly expressed in pituitary and urophysis, *Endocrinology 142*, 446−454.
11. Miller, D. B., and O'Callaghan, J. P. (2002) Neuroendocrine aspects of the response to stress, *Metabolism 51*, 5−10.
12. Vale, W., Spiess, J., Rivier, C., and Rivier, J. (1981) Characterization of a 41-residue ovine hypothalamic peptide that stimulates secretion of corticotropin and beta-endorphin, *Science 213*, 1394−1397.
13. Raffin-Sanson, M. L., de Keyzer, Y., and Bertagna, X. (2003) Proopiomelanocortin, a polypeptide precursor with multiple functions: from physiology to pathological conditions, *Eur. J. Endocrinol. 149*, 79−90.
14. Perrin, M. H., Sutton, S., Bain, D. L., Berggren, W. T., and Vale, W. W. (1998) The first extracellular domain of corticotropin releasing factor-R1 contains major binding determinants for urocortin and astressin, *Endocrinology 139*, 566−570.
15. Dautzenberg, F. M., Wille, S., Lohmann, R., and Spiess, J. (1998) Mapping of the ligand-selective domain of the *Xenopus laevis* corticotropin-releasing factor receptor 1: implications for the ligand-binding site, *Proc. Natl. Acad. Sci. U.S.A. 95*, 4941−4946.
16. Dautzenberg, F. M., Kilpatrick, G. J., Wille, S., and Hauger, R. L. (1999) The ligand-selective domains of corticotropin-releasing factor type 1 and type 2 receptor reside in different extracellular domains: generation of chimeric receptors with a novel ligand-selective profile, *J. Neurochem. 73*, 821−829.
17. Wille, S., Sydow, S., Palchaudhuri, M. R., Spiess, J., and Dautzenberg, F. M. (1999) Identification of amino acids in the N-terminal domain of corticotropin-releasing factor receptor 1 that are important determinants of high-affinity ligand binding, *J. Neurochem. 72*, 388−395.
18. Assil, I. Q., Qi, L. J., Arai, M., Shomali, M., and Abou-Samra, A. B. (2001) Juxtamembrane region of the amino terminus of the corticotropin releasing factor receptor type 1 is important for ligand interaction, *Biochemistry 40*, 1187−1195.
19. Liaw, C. W., Grigoriadis, D. E., Lorang, M. T., De Souza, E. B., and Maki, R. A. (1997) Localization of agonist- and antagonist-binding domains of human corticotropin-releasing factor receptors, *Mol. Endocrinol. 11*, 2048−2053.
20. Hoare, S. R., Sullivan, S. K., Pahuja, A., Ling, N., Crowe, P. D., and Grigoriadis, D. E. (2003) Conformational states of the

corticotropin releasing factor 1 (CRF1) receptor: detection, and pharmacological evaluation by peptide ligands, *Peptides 24*, 1881−1897.
21. Perrin, M. H., and Vale, W. W. (1999) Corticotropin releasing factor receptors and their ligand family, *Ann. N.Y. Acad. Sci. 885*, 312−328.
22. Ruhmann, A., Bonk, I., and Kopke, A. K. (1999) High-affinity binding of urocortin and astressin but not CRF to G protein-uncoupled CRFR1, *Peptides 20*, 1311−1319.
23. Grace, C. R., Perrin, M. H., DiGruccio, M. R., Miller, C. L., Rivier, J. E., Vale, W. W., and Riek, R. (2004) NMR structure and peptide hormone binding site of the first extracellular domain of a type B1 G protein-coupled receptor, *Proc. Natl. Acad. Sci. U.S.A. 101*, 12836−12841.
24. Klose, J., Fechner, K., Beyermann, M., Krause, E., Wendt, N., Bienert, M., Rudolph, R., and Rothemund, S. (2005) Impact of N-terminal domains for corticotropin-releasing factor (CRF) receptor−ligand interactions, *Biochemistry 44*, 1614−1623.
25. Dohlman, H. G., Caron, M. G., Strader, C. D., Amlaiky, N., and Lefkowitz, R. J. (1988) Identification and sequence of a binding site peptide of the beta 2-adrenergic receptor, *Biochemistry 27*, 1813−1817.
26. Janovick, J. A., Haviv, F., Fitzpatrick, T. D., and Conn, P. M. (1993) Differential orientation of a GnRH agonist and antagonist in the pituitary GnRH receptor, *Endocrinology 133*, 942−945.
27. Kennedy, A. P., Mangum, K. C., Linden, J., and Wells, J. N. (1996) Covalent modification of transmembrane span III of the A1 adenosine receptor with an antagonist photoaffinity probe, *Mol. Pharmacol. 50*, 789−798.
28. Li, Y. M., Marnerakis, M., Stimson, E. R., and Maggio, J. E. (1995) Mapping peptide-binding domains of the substance P (NK-1) receptor from P388D1 cells with photolabile agonists, *J. Biol. Chem. 270*, 1213−1220.
29. Boucard, A. A., Sauve, S. S., Guillemette, G., Escher, E., and Leduc, R. (2003) Photolabelling the rat urotensin II/GPR14 receptor identifies a ligand-binding site in the fourth transmembrane domain, *Biochem. J. 370*, 829−838.
30. Boucard, A. A., Wilkes, B. C., Laporte, S. A., Escher, E., Guillemette, G., and Leduc, R. (2000) Photolabeling identifies position 172 of the human AT(1) receptor as a ligand contact point: receptor-bound angiotensin II adopts an extended structure, *Biochemistry 39*, 9662−9670.
31. Behar, V., Bisello, A., Rosenblatt, M., and Chorev, M. (1999) Direct identification of two contact sites for parathyroid hormone (PTH) in the novel PTH-2 receptor using photoaffinity cross-linking, *Endocrinology 140*, 4251−4261.
32. Behar, V., Bisello, A., Bitan, G., Rosenblatt, M., and Chorev, M. (2000) Photoaffinity cross-linking identifies differences in the interactions of an agonist and an antagonist with the parathyroid hormone/parathyroid hormone-related protein receptor, *J. Biol. Chem. 275*, 9−17.
33. Dong, M., Pinon, D. I., Cox, R. F., and Miller, L. J. (2004) Importance of the amino terminus in secretin family G protein-coupled receptors. Intrinsic photoaffinity labeling establishes initial docking constraints for the calcitonin receptor, *J. Biol. Chem. 279*, 1167−1175.
34. Dong, M., Pinon, D. I., Cox, R. F., and Miller, L. J. (2004) Molecular approximation between a residue in the amino-terminal region of calcitonin and the third extracellular loop of the class B G protein-coupled calcitonin receptor, *J. Biol. Chem. 279*, 31177−31182.
35. Tan, Y. V., Couvineau, A., Van Rampelbergh, J., and Laburthe, M. (2003) Photoaffinity labeling demonstrates physical contact between vasoactive intestinal peptide and the N-terminal ectodomain of the human VPAC1 receptor, *J. Biol. Chem. 278*, 36531−36536.
36. Tan, Y. V., Couvineau, A., and Laburthe, M. (2004) Diffuse pharmacophoric domains of vasoactive intestinal peptide (VIP) and further insights into the interaction of VIP with the N-terminal ectodomain of human VPAC1 receptor by photoaffinity labeling with [Bpa6]-VIP, *J. Biol. Chem. 279*, 38889−38894.
37. Pham, V. I., and Sexton, P. M. (2004) Photoaffinity scanning in the mapping of the peptide receptor interface of class II G protein-coupled receptors, *J. Pept. Sci. 10*, 179−203.
38. Assil-Kishawi, I., and Abou-Samra, A. B. (2002) Sauvagine cross-links to the second extracellular loop of the corticotropin-releasing factor type 1 receptor, *J. Biol. Chem. 277*, 32558−32561.
39. Beyermann, M., Fechner, K., Furkert, J., Krause, E., and Bienert, M. (1996) A single-point slight alteration set as a tool for structure−activity relationship studies of ovine corticotropin releasing factor, *J. Med. Chem. 39*, 3324−3330.
40. Fraker, P. J., and Speck, J. C., Jr. (1978) Protein and cell membrane iodinations with a sparingly soluble chloroamide, 1,3,4,6-tetrachloro-3a,6a-diphrenylglycoluril, *Biochem. Biophys. Res. Commun. 80*, 849−857.
41. Wietfeld, D., Heinrich, N., Furkert, J., Fechner, K., Beyermann, M., Bienert, M., and Berger, H. (2004) Regulation of the coupling to different G proteins of rat corticotropin-releasing factor receptor type 1 in human embryonic kidney 293 cells, *J. Biol. Chem. 279*, 38386−38394.
42. Laemmli, U. K. (1970) Cleavage of structural proteins during the assembly of the head of bacteriophage T4, *Nature 227*, 680−685.
43. Grigoriadis, D. E., and De Souza, E. B. (1989) Heterogeneity between brain and pituitary corticotropin-releasing factor receptors is due to differential glycosylation, *Endocrinology 125*, 1877−1888.
44. Assil, I. Q., and Abou-Samra, A. B. (2001) N-glycosylation of CRF receptor type 1 is important for its ligand-specific interaction, *Am. J. Physiol. Endocrinol. Metab. 281*, E1015−E1021.
45. Hoare, S. R., Sullivan, S. K., Fan, J., Khongsaly, K., and Grigoriadis, D. E. (2005) Peptide ligand binding properties of the corticotropin-releasing factor (CRF) type 2 receptor: pharmacology of endogenously expressed receptors, G-protein-coupling sensitivity and determinants of CRF2 receptor selectivity, *Peptides 26*, 457−470.
46. Adams, A. E., Bisello, A., Chorev, M., Rosenblatt, M., and Suva, L. J. (1998) Arginine 186 in the extracellular N-terminal region of the human parathyroid hormone 1 receptor is essential for contact with position 13 of the hormone, *Mol. Endocrinol. 12*, 1673−1683.
47. Bisello, A., Adams, A. E., Mierke, D. F., Pellegrini, M., Rosenblatt, M., Suva, L. J., and Chorev, M. (1998) Parathyroid hormone-receptor interactions identified directly by photocross-linking and molecular modeling studies, *J. Biol. Chem. 273*, 22498−22505.
48. Dong, M., Wang, Y., Pinon, D. I., Hadac, E. M., and Miller, L. J. (1999) Demonstration of a direct interaction between residue 22 in the carboxyl-terminal half of secretin and the amino-terminal tail of the secretin receptor using photoaffinity labeling, *J. Biol. Chem. 274*, 903−909.
49. Dong, M., Wang, Y., Hadac, E. M., Pinon, D. I., Holicky, E., and Miller, L. J. (1999) Identification of an interaction between residue 6 of the natural peptide ligand and a distinct residue within the amino-terminal tail of the secretin receptor, *J. Biol. Chem. 274*, 19161−19167.
50. Dong, M., Asmann, Y. W., Zang, M., Pinon, D. I., and Miller, L. J. (2000) Identification of two pairs of spatially approximated residues within the carboxyl terminus of secretin and its receptor, *J. Biol. Chem. 275*, 26032−26039.
51. Pham, V., Wade, J. D., Purdue, B. W., and Sexton, P. M. (2004) Spatial proximity between a photolabile residue in position 19 of salmon calcitonin and the amino terminus of the human calcitonin receptor, *J. Biol. Chem. 279*, 6720−6729.

BI0507027